Inorg. Chem. **2008**, *47*, 10935−10944

One- and Two-Electron Reduced 1,2-Diketone Ligands in $[Cr^{III}(L^{\bullet})_3]$ ($S = 0$) and $Na_2(Et_2O)_2[V^{IV}(L^{Red})_3]$ ($S = {}^1/_2$)

Geoffrey H. Spikes, Stephen Sproules, Eckhard Bill, Thomas Weyhermüller, and Karl Wieghardt*

Max-Planck-Institut für Bioanorganische Chemie, Stiftstrasse 34−36, 45470 Mülheim an der Ruhr, Germany

Received June 17, 2008

The electronic structures of chromium and vanadium centers coordinated by three reduced 1,2-diketones have been elucidated by using density functional theory (DFT) calculations and a host of physical methods: X-ray crystallography; cyclic voltammetry; ultraviolet−visible (UV−vis), nuclear magnetic resonance (NMR), and electron paramagnetic resonance (EPR) spectroscopy; and magnetic susceptibility measurements. The metal center in octahedral $[Cr^{III}(L^{\bullet})_3]^0$ (**1**), a Cr^{III} (d^3) ion is coupled antiferromagnetically to three monoanionic ligand π-radicals affording an $S = 0$ ground state. In contrast, $Na_2(Et_2O)_2[V^{IV}(L^{Red})_3]$ (**2**) ($S = {}^1/_2$), possesses a central V^{IV} (d^1) ion *O,O′*-coordinated to three closed-shell, doubly reduced ligands which in turn are coordinated by two Na cations enforcing a trigonal prismatic geometry at the vanadium center. **2** can be oxidized electrochemically by one and two electrons generating a monoanion, $[V(L)_3]^{1-}$, and a neutral species, $[V(L)_3]^0$, respectively. DFT calculations at the B3LYP level show that the one-electron oxidized product contains an octahedral V^{IV} ion coupled antiferromagnetically to one monoanionic ligand π-radical $[V^{IV}(L^{\bullet})(L^{Red})_2]^{1-}$ ($S = 0$). In contrast, the two-electron oxidized product contains a V^{III} ion coupled antiferromagnetically to three ligand π-radicals in an octahedral field $[V^{III}(L^{\bullet})_3]^0$ ($S = {}^1/_2$).

Introduction

Recently there has been resurgent interest in redox noninnocent ligands because of their identification in many highly reactive catalytic species,[1−6] of which archetypal examples include complexes based on the catechol (cat), 1,2-benzosemiquinone (SQ), and 1,2-benzoquinone (BQ) redox series.[7,8] Surprisingly, while this redox activity is now well understood for the later transition metals, the charge distribution in vanadium quinone complexes is still discussed controversially. For example, a reversible two-electron oxidation series has been identified for $[V^{IV}(cat)_3]^{2-}$, where cat^{2-} represents the catecholate dianion, that is oxidized to a neutral species through a monoanionic intermediate. However, the nature of the first monoanionic oxidation product, whether metal-based to give V^V or ligand-based to give V^{IV} with one radical ligand, remains unclear.[9,10] The identity of the neutral species is also uncertain. Its electronic structure has been assigned as V^{III} with three π-radical ligands in the solid state, but has been suggested to rearrange to V^V in solution.[10] Furthermore, it has been inferred that these hard ligands will tend to stabilize the highest possible oxidation state of the metal center.[9]

Until very recently, the equivalent redox versatility had not been observed for acyclic 1,2-diketones with no known examples of complexes with coordinated 1,2-diketone radical ligands. Early transition metal complexes, containing 1,2-diketones in their two-electron reduced diolate form, have

* To whom correspondence should be addressed. E-mail: wieghardt@mpi-muelheim.mpg.de. Fax: 49-208-306-3952.

(1) Grützmacher, H. *Angew. Chem., Int. Ed.* **2008**, *47*, 1814.
(2) Rolle, C. J., III; Hardcastle, K. I.; Soper, J. D. *Inorg. Chem.* **2008**, *47*, 1892.
(3) Blackmore, K. J.; Lal, N.; Ziller, J. W.; Heyduk, A. F. *J. Am. Chem. Soc.* **2008**, *130*, 2728.
(4) Bart, S. C.; Chlopek, K.; Bill, E.; Boukamp, M. W.; Lobkovsky, E.; Wieghardt, K.; Chirik, P. *J. Am. Chem. Soc.* **2006**, *128*, 13901.
(5) Knijnenburg, Q.; Gambarotta, S.; Budzelaar, P. H. M. *Dalton Trans.* **2006**, 5442.
(6) Jones, G. D.; Martin, J. L.; McFarland, C.; Allen, O. R.; Hall, R. E.; Haley, A. D.; Brandon, R. J.; Konovalova, T.; Desrochers, P. J.; Pulay, P.; Vicic, D. A. *J. Am. Chem. Soc.* **2006**, *128*, 13175.
(7) Pierpont, C. G.; Lange, C. W. *Prog. Inorg. Chem.* **1994**, *41*, 331.
(8) Chaudhuri, P.; Wieghardt, K. *Prog. Inorg. Chem.* **2001**, *50*, 151.
(9) Cooper, S. R.; Koh, Y. B.; Raymond, K. N. *J. Am. Chem. Soc.* **1982**, *104*, 5092.
(10) Cass, M. E.; Gordon, N. R.; Pierpont, C. G. *Inorg. Chem.* **1986**, *25*, 3962.

10.1021/ic801122m CCC: $40.75
Published on Web 10/29/2008

Scheme 1. Observed Redox States and Bond Lengths for Bulky 1,2-Diketone Bis(2,6-diisopropylphenyl)glyoxal

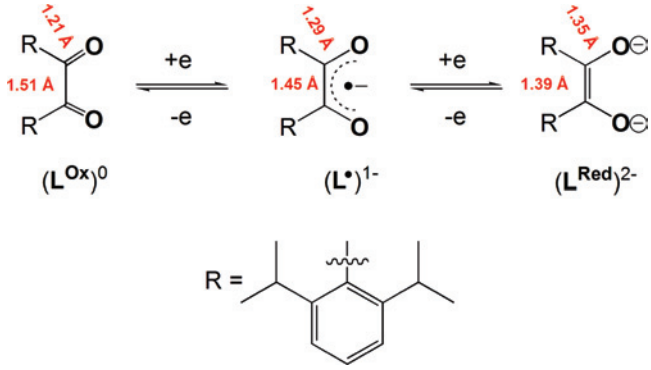

Scheme 2. Synthesis of $[Cr^{III}(L^{\bullet})_3]$ (**1**) and $Na_2(Et_2O)_2[V^{IV}(LRed)_3]$ (**2**)

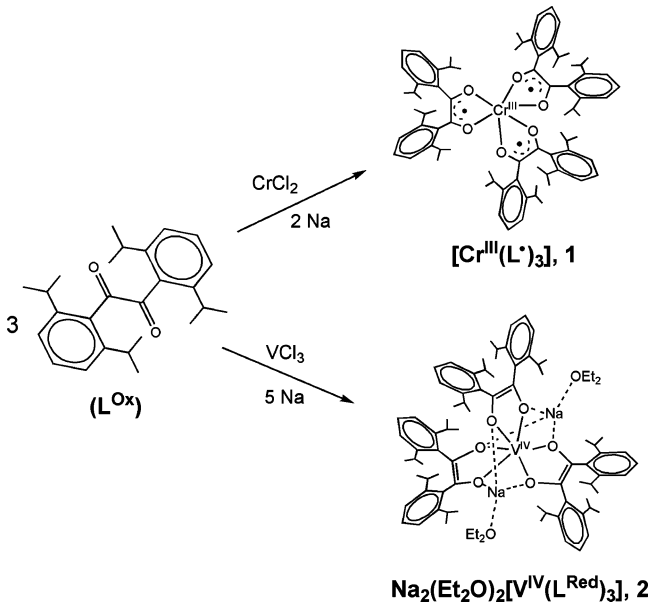

been reported,[11−15] as has one example of a ligating neutral benzyl.[16] We have shown that the bulky diaryl 1,2-diketone bis(2,6-diisopropylphenyl)glyoxal $(L^{Ox})^0$ is a redox active ligand (L) that can form complexes in its doubly reduced, closed-shell $(L^{Red})^{2-}$ state or as a singly reduced radical anion $(L^{\bullet})^{1-}$ with mid-to-late transition metal ions (Scheme 1).[17,18]

Complexes containing $(L^{Red})^{2-}$ or $(L^{\bullet})^{1-}$ have been accessed via reduction of the corresponding metal halide with sodium in the presence of the free 1,2-diketone ligand (Scheme 2). This free acyclic ligand is significantly harder to reduce than 1,2-benzoquinone and its derivatives, as is shown by their respective redox potentials (Scheme 3).

Scheme 3. First Reduction Potentials for 1,2-Benzoquinone and $(L^{Ox})^0$ in Acetonitrile[19]

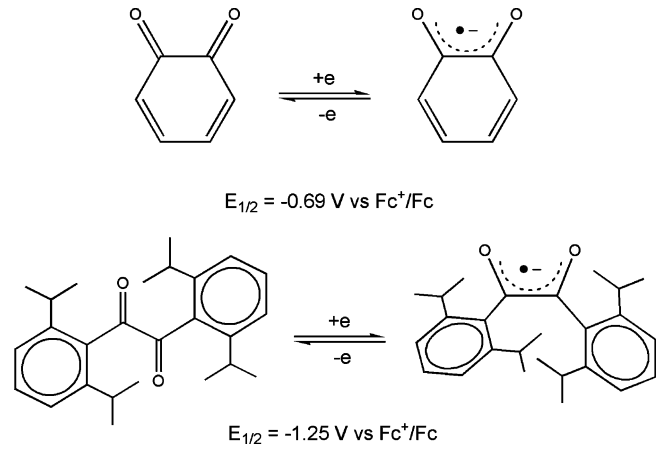

In two previous reports[17,18] we have established that it is possible to distinguish the ligand oxidation levels (Scheme 1) by their varying C—O and C—C distances, using high-quality X-ray crystallography. Herein, we report the isolation and structural characterization of two, six-coordinate, early transition metal complexes with very different ligand and metal oxidation levels, namely, octahedral $[Cr^{III}(L^{\bullet})_3]$ (**1**) and trigonal prismatic $Na_2(Et_2O)_2[V^{IV}(LRed)_3]$ (**2**) with a detailed electrochemical and density functional theory (DFT) investigation of the redox chemistry of **2**.

Experimental Section

All syntheses were carried out using standard glovebox and Schlenk techniques in the absence of water and dioxygen. Solvents were purchased from Fluka and dried over 4 Å molecular sieves. Benzene-d_6 was purchased from Cambridge Isotope Laboratories, Inc., degassed via repeated freeze−pump−thaw cycles, and dried over 4 Å molecular sieves. Sodium metal was purchased from Aldrich and washed with hexanes prior to use. The reagents $CrCl_2$ and VCl_3 were purchased from Strem and used without further purification. The neutral 1,2-diketone ligand, bis(2,6-diisopropylphenyl)glyoxal, was prepared by the literature method.[17]

$[Cr^{III}(L^{\bullet})_3]$ (1). A solution of bis(2,6-diisopropylphenyl)glyoxal (200 mg, 0.52 mmol) in Et_2O (15 mL) was added while stirring to $CrCl_2$ (21 mg, 0.17 mmol) and Na (8 mg, 0.35 mmol). The pale yellow solution turned a deep orange-red color over 24 h. Removal of the solvent in vacuo resulted in a dark red residue that was extracted in Et_2O (6 mL) and filtered. Slow evaporation yielded **1** as dark red crystals. Yield: 125 mg (62%).

Anal. Calcd for $C_{78}H_{102}O_6Cr$: C, 78.9; H, 8.66. Found: C, 78.5; H, 8.62. UV−vis (C_6H_6): 758 (sh, 2400), 727 (sh, 1600), 696 (sh, 1300), 542 (4300), 470 (17800), 454 (sh, 12700), 360 nm (8900 M^{-1} cm^{-1}). ^1H NMR (C_6D_6): δ 0.84 [br, d, 18H, $CH(CH_3)_2$], 1.22 [d, 32H, $J = 6.9$ Hz, $CH(CH_3)_2$], 1.41 [br, d, 9H, $CH(CH_3)_2$], 1.88 [br, sept, 12H, $CH(CH_3)_2$], 3.56 [br, d, 9H, $J = 6.9$ Hz, $CH(CH_3)_2$], 6.59 (br, d, 6H, Ar-**H**), 7.51 (br, d, 6H, Ar-**H**), 7.80 (br, t, 6H,

(11) Hofmann, P.; Frede, M.; Stauffert, P.; Lasser, W.; Thewalt, U. *Angew. Chem., Int. Ed.* **1985**, *24*, 712.
(12) Erker, G.; Czisch, P.; Schlund, R.; Angermund, K.; Krüger, C. *Angew. Chem., Int. Ed.* **1986**, *25*, 364.
(13) Song, L.-C.; Liu, P.-C.; Han, C.; Hu, Q.-M. *J. Organomet. Chem.* **2002**, *648*, 119.
(14) Chisholm, M. H.; Huffman, J. C.; Ratermann, A. L. *Inorg. Chem.* **1983**, *22*, 4100.
(15) Sugawara, K.-L.; Hikichi, S.; Akita, M. *Dalton Trans.* **2002**, 4514.
(16) Carofiglio, T.; Cozzi, P. G.; Floriani, C.; Chiesi-Villa, A.; Rizzolo, C. *Organometallics* **1993**, *12*, 2726.
(17) Spikes, G. H.; Bill, E.; Weyhermüller, T.; Wieghardt, K. *Chem. Commun.* **2007**, 4339.
(18) Spikes, G. H.; Bill, E.; Weyhermüller, T.; Wieghardt, K. *Angew. Chem., Int. Ed.* **2008**, *47*, 2973.
(19) The $E_{1/2}$ for 1,2-benzosemiquinone from: Stallings, M. D.; Morrison, M. M.; Sawyer, D. T. *Inorg. Chem.* **1981**, *20*, 2655; was referenced to Fc using the conversion Fc = +0.38 V versus SCE (MeCN/$[NEt_4][ClO_4]$) from: Connelly, N. G.; Geiger, W. E. *Chem. Rev.* **1996**, *96*, 877. For the $E_{1/2}$ measurement of $(L^{Ox})^0$ see Supporting Information.

Table 1. Crystallographic Data for **1** and **2**

	1	**2**
chemical formula	$C_{78}H_{102}O_6Cr$	$C_{86}H_{122}Na_2O_8V$
crystal size (mm^3)	0.40 × 0.24 × 0.20	0.18 × 0.06 × 0.06
F_W	1187.60	1380.76
space group	*C*2/*c* (No. 15)	*Pbcn* (No. 60)
a (Å)	10.8701(3)	23.3861(6)
b (Å)	27.5230(7)	18.7470(4)
c (Å)	23.5899(6)	18.1395(4)
α (deg)	90	90
β (deg)	92.448(3)	90
γ (deg)	90	90
V (Å^3)	7051.1(3)	7952.7(3)
Z	4	4
T (K)	100(2)	100(2)
ρ calcd (g cm^{-3})	1.119	1.153
reflns collected/$2\Theta_{max}$	86908/33.27	147284/30.0
unique reflns/$I > 2\sigma(I)$	13550/11070	11566/9382
no. of params/restraints	408/4	454/8
λ (Å)/*μ*(Mo Kα) (cm^{-1})	0.71073/2.12	0.71073/1.89
R1[a]/GOF[b]	0.0445/1.019	0.0444/1.061
wR2[c] ($I > 2\sigma(I)$)	0.1140	0.01063
residual density (e $Å^{-3}$)	+0.848/−0.987	+0.373/−0.348

[a] Observation criterion: $I > 2\sigma(I)$. $R1 = \sum F_o| - |F_c|/\sum|F_o|$. [b] $GOF = [\sum[w(F_o^2 - F_c^2)^2]/(n-p)]^{1/2}$. [c] $wR2 = [\sum[w(F_o^2 - F_c^2)^2]/\sum[w(F_o^2)^2]]^{1/2}$, where $w = 1/\sigma^2(F_o^2) + (aP)^2 + bP$, $P = (F_o^2 + 2F_c^2)/3$.

Ar-**H**). ^{13}C NMR (C_6D_6): *δ* 21.4 [CH(**C**H_3)$_2$], 23.5 [CH(**C**H_3)$_2$], 25.6 [CH(**C**H_3)$_2$], 28.5 [**C**H(CH_3)$_2$], 29.2 [**C**H(CH_3)$_2$], 30.6 [**C**H(CH_3)$_2$], 67.6 (Ar**C**O), 120.6, 122.7, 132.5. Electrospray mass spectrum (ESI): M^+ *m*/*z* 1186, (1%), *m*/*z* 189, (COC_6H_3-2,6-^{i}Pr$_2$, 100%).

$Na_2(Et_2O)_2[V^{IV}(L^{Red})_3]$ (2). A solution of bis(2,6-diisopropylphenyl)glyoxal (200 mg, 0.52 mmol) in Et_2O (20 mL) was added while stirring to VCl_3 (27 mg, 0.17 mmol) and Na (20 mg, 0.87 mmol). The pale yellow solution turned a deep purple color over 24 h. Removal of the solvent in vacuo resulted in a dark blue residue that was extracted in Et_2O (5 mL) and filtered. Slow evaporation yielded **2** as dark purple crystals. Yield: 77 mg (33%).

Anal. Calcd for $C_{86}H_{122}Na_2O_8V$: C, 74.8; H, 8.91. Found: C, 74.5; H, 8.79. UV−vis (Et_2O): 870 (sh, 3200), 725 (4700), 485 (sh, 6500), 365 nm (8600 M^{-1} cm^{-1}). ESI mass spectrum: *m*/*z* 189, (COC_6H_3-2,6-^{i}Pr$_2$, 100%).

X-Ray Crystallographic Data Collection and Refinement of Structures. A dark red single crystal of **1** and a purple crystal of **2** were coated with perfluoropolyether, picked up with nylon loops, and mounted in the nitrogen cold stream of the diffractometer. A Bruker-Nonius KappaCCD diffractometer equipped with a Mo-target rotating-anode X-ray source and a graphite monochromator (Mo Kα, $\lambda = 0.71073$ Å) was used. Final cell constants were obtained from least-squares fits of all measured reflections. The structures were readily solved by direct methods and subsequent difference Fourier techniques. The Siemens SHELXTL[20] software package was used for solution and artwork of the structure, and SHELXL97[21] was used for the refinement. All non-hydrogen atoms were refined anisotropically. Hydrogen atoms were placed at calculated positions and refined as riding atoms with isotropic displacement parameters. Crystallographic data of the compounds are listed in Table 1, and selected bond distances and angles are published in Table 2.

Physical Measurements. Electronic absorption spectra were recorded with a Perkin-Elmer Lambda 19 double-beam photometer (300−2000 nm), and spectra from spectroelectrochemical measurements were recorded with an HP 8452A diode-array spectrophotometer (200−1100 nm). Cyclic voltammograms were recorded with an EG&G potentiostat/galvanostat in 1:1 CH_2Cl_2/Et_2O solutions (0.10 M [N(*n*-Bu)$_4$]PF_6) at a glassy carbon working electrode. Ferrocene was used as an internal standard; all redox potentials are given versus the ferrocenium/ferrocene (Fc^+/Fc) couple. Temperature-dependent magnetic susceptibilities were measured by using a SQUID magnetometer (MPMS Quantum Design) at 1.0 T (4−300 K). Underlying diamagnetism was corrected by using tabulated Pascal's constants. X-band EPR spectra were recorded on a Bruker ESP 300 spectrometer. NMR spectra were recorded on Varian Mercury 400 MHz instrument at ambient temperature.

Calculations. All calculations were done with the ORCA program package.[22] The geometry optimizations were carried out at either the B3LYP[23] or BP86[24] levels of DFT. The all-electron Gaussian basis sets used were those reported by the Ahlrichs group.[25,26] For chromium, vanadium, sodium, and oxygen atoms, the triple-ζ-quality basis sets with one set of polarization functions were used (TZVP).[25] The carbon and hydrogen atoms were described by using smaller polarized split-valence SV(P) basis sets that are double-ζ-quality in the valence region with a polarizing set of d-functions on the non-hydrogen atoms.[26] The auxiliary basis sets for all atoms used to expand the electron density in the calculations were chosen to match the orbital basis. The self-consistent field (SCF) calculations were tightly converged: 1×10^{-8} E_h in energy, 1×10^{-7} E_h in the density change, and 1×10^{-7} in the maximum element of the DIIS[27] error vector. The geometric search for all complexes was carried out in redundant internal coordinates without imposing geometry constraints. The geometries were considered converged after the energy change was less than 5×10^{-6} E_h, the gradient norm and maximum gradient element were smaller than 1×10^{-4} and 3×10^{-4} E_h/Bohr, respectively, and the root-mean-square and maximum displacements of the atoms were smaller than 2×10^{-3} and 4×10^{-3} Bohr, respectively. Corresponding[28] and quasi-restricted[29] orbitals and density plots were obtained with Molekel.[30] We used the broken symmetry (BS) approach to describe our computational results for **1** and for the one- and two-electron oxidized complexes of **2** containing noninnocent ligands.[4,31−33]

(20) *SHELXTL*, version 5; Siemens Analytical X-ray Instruments, Inc.: Madison, WI, 1994.

(21) Sheldrick, G. M. *SHELXL97*; University of Göttingen: Göttingen, Germany, 1997.

(22) Neese, F. *Orca, an Ab Initio, Density Functional and Semiempirical Electronic Structure Program Package*, version 2.6, revision 35; Institut für Physikalische und Theoretische Chemie, Universität Bonn: Bonn, Germany, 2008.

(23) (a) Becke, A. D. *J. Chem. Phys.* **1993**, *98*, 5648. (b) Lee, C. T.; Yang, W. T.; Parr, R. G. *Phys. Rev. B* **1988**, *37*, 785.

(24) (a) Becke, A. D. *J. Chem. Phys.* **1986**, *84*, 4524. (b) Perdew, J. P. *Phys. Rev. B* **1986**, *33*, 8822.

(25) Schäfer, A.; Horn, H.; Ahlrichs, R. *J. Chem. Phys.* **1992**, *97*, 2751.

(26) Schäfer, A.; Huber, C.; Ahlrichs, R. *J. Chem. Phys.* **1994**, *100*, 5829.

(27) (a) Pulay, P. *Phys. Chem. Lett.* **1980**, *73*, 393. (b) Pulay, P. *J. Comput. Chem.* **1992**, *3*, 556.

(28) Neese, F. *J. Phys. Chem. Solids* **2004**, *65*, 781.

(29) Schöneboon, J. C.; Neese, F.; Thiele, W. *J. Am. Chem. Soc.* **2005**, *127*, 5840.

(30) *Molekel, Advanced Interactive 3D-Graphics for Molecular Sciences*, Swiss National Supercomputing Centre. http://www.cscs.ch/molekel.

(31) Noodleman, L.; Peng, C. Y.; Case, D. A.; Monesca, J. M. *Coord. Chem. Rev.* **1995**, *144*, 199.

(32) (a) Noodleman, L. *J. Chem. Phys.* **1981**, *74*, 5737. (b) Noodleman, L.; Case, D. A.; Aizman, A. *J. Am. Chem. Soc.* **1988**, *110*, 1001. (c) Noodleman, L.; Davidson, E. R. *Chem. Phys.* **1986**, *109*, 131. (d) Noodleman, L.; Norman, J. G.; Osborne, J. H.; Aizman, A.; Case, D. A. *J. Am. Chem. Soc.* **1985**, *107*, 3418.

(33) Kapre, R. R.; Bothe, E.; Weyhermüller, T.; DeBeer George, S.; Muresan, N.; Wieghardt, K. *Inorg. Chem.* **2007**, *46*, 7827.

Table 2. Selected Bond Distances (Å) and Angles (deg) in **1** and **2**

		Complex **1**			
Cr—O1	1.949(1)	O1—C1	1.299(1)	C1—C2	1.417(1)
Cr—O2	1.938(1)	O2—C2	1.298(1)	C31—C31′	1.416(2)
Cr—O31	1.947(1)	O31—C31	1.296(1)		
O1—Cr—O2	79.80(3)	O1′—Cr—O2′	79.80(3)	O1—Cr—O31′	163.59(3)
O31—Cr—O31′	79.57(4)	O1′—Cr—O31	163.59(3)	O2—Cr—O2′	164.73(4)
		Complex **2**			
V—O1	1.959(1)	O1—C1	1.368(1)	C1—C2	1.357(2)
V—O2	1.962(1)	O2—C2	1.367(1)	C31—C31′	1.360(2)
V—O31	1.958(1)	O31—C31	1.367(1)	O1—Na1	2.321(1)
O2′—Na1	2.277(1)	O31—Na1	2.301(1)	Na1—O51	2.382(1)
O1—V—O2	77.93(3)	O1—V—O31	84.87(3)	O1—V—O1′	138.49(5)
O31—V—O31′	77.93(5)	O1—V—O2′	84.65(4)	O1—V1—O31′	129.83(3)
O1′—V—O2′	77.93(3)	O2′—V—O31	84.87(3)		

Results and Discussion

The addition of a solution composed of 3 equiv of bis(2,6-diisopropylphenyl)glyoxal (L^{Ox}) in Et_2O at about 25 °C to 1 equiv of anhydrous $CrCl_2$ and 2 equiv of Na while stirring led to a gradual color change from pale yellow to deep orange over the course of 24 h. Filtration, followed by removal of the solvent in vacuo, yielded a dark orange-red powder. Subsequent recrystallization from Et_2O gave dark red plates of neutral **1** (Figure 1), which were suitable for single-crystal X-ray diffraction, in moderate yield (~62%). Similarly, the addition of 3 equiv of L^{Ox} in Et_2O at about 25 °C to 1 equiv of anhydrous VCl_3 and 5 equiv of Na while stirring led to a color change of deep purple over the course of 24 h. Filtration, followed by removal of the solvent in vacuo, yielded a purple powder. Subsequent recrystallization from Et_2O gave dark purple plates of **2** (Figure 2), suitable for single-crystal X-ray diffraction in low yield (~33%).

The CrO_6 polyhedron in **1** is octahedral as in the previously reported tris(1,2-diketonato)iron(III) complex $[Fe^{III}(L^{\bullet})_3]$.[18] The carbon—oxygen and carbon—carbon bond lengths at 1.296(1)—1.299(1) and 1.416(2)—1.417(1) Å, respectively, indicate the presence of three radical anions, $(L^{\bullet})^{1-}$. The chromium—oxygen bond lengths are typical of Cr^{III}.[34,35] This is the first example of an early transition metal complex with 1,2-diketone radical anion ligands $[Cr^{III}(L^{\bullet})_3]^0$.

In contrast, the ligand environment around the vanadium center in **2** approximates trigonal prismatic geometry (Figure 3) as is clearly established by the small trigonal twist angle (Θ) of 6.1°, compared to the 60° twist angle in an octahedron and the 0° twist angle in a trigonal prism. The short glyoxal carbon—carbon bond length and the long carbon—oxygen bond lengths of 1.357(1)—1.360(1) and 1.367(1) Å, respectively, are indicative of the doubly reduced enediolate form (Scheme 1).[9] The mean value of the six V—O bond distances of 1.959 Å is consistent with the V^{IV} oxidation state and is similar to the analogous vanadium(IV) catecholate complex $[Et_3NH]_2[V^{IV}(cat)_3]\cdot CH_3CN$ (av 1.930 Å). Here the VO_6 polyhedron is more octahedral with a twist angle of 38.6°.[9] The strikingly different geometry of these two V^{IV} complexes appears to be counterion based; in **2** there are six further close contacts at 2.277(1)—2.321(1) Å between the glyoxal donor oxygens and two Na cations each capping a face of the trigonal prism. The coordination environment around these four-coordinate Na ions is completed by an O-coordinated diethylether ligand.

$[Cr^{III}(L^{\bullet})_3]$ (**1**) is diamagnetic as determined from its ^1H NMR and ^{13}C NMR spectra (Experimental Section). Its electronic spectrum recorded in C_6H_6 (Figure 4) resembles those recorded for tris(semiquinonate)[36—39] and tris(phenoxyl)chromium(III) complexes.[40] The sharp peak at 542 nm (ε = 3200 M^{-1} cm^{-1}) can be ascribed to a spin forbidden $^4A_{2g} \rightarrow {}^2E_g$ transition corresponding to a spin flip in the

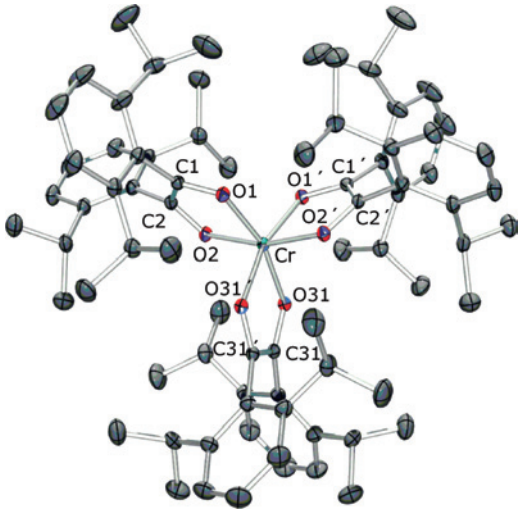

Figure 1. Structure of the neutral complex $[Cr^{III}(L^{\bullet})_3]$ in single crystals of **1**. Thermal ellipsoids are drawn at 50% probability.

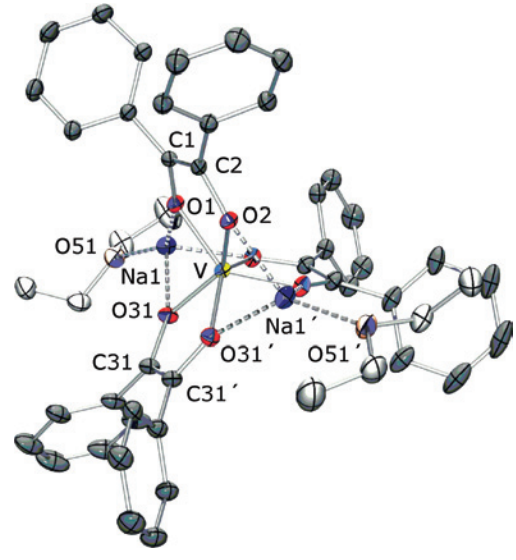

Figure 2. Structure of the neutral complex $Na_2(Et_2O)_2[V^{IV}(L^{Red})_3]$ in single crystals of **2**. Isopropyl substituents have been omitted for clarity, and thermal ellipsoids are drawn at 50% probability.

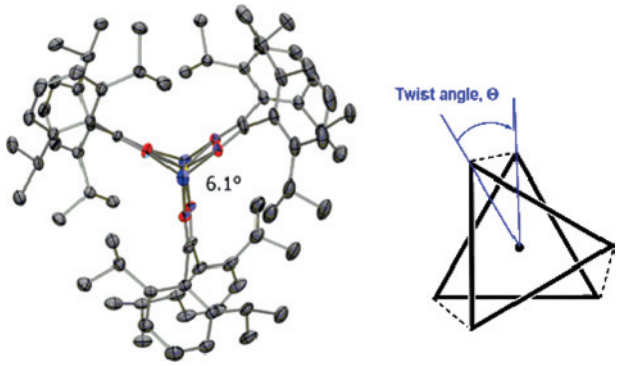

Figure 3. View of **2** down the C_3 axis showing Na atoms in blue; coordinating Et_2O molecules are not shown. The definition of the twist angle, Θ, is also shown.

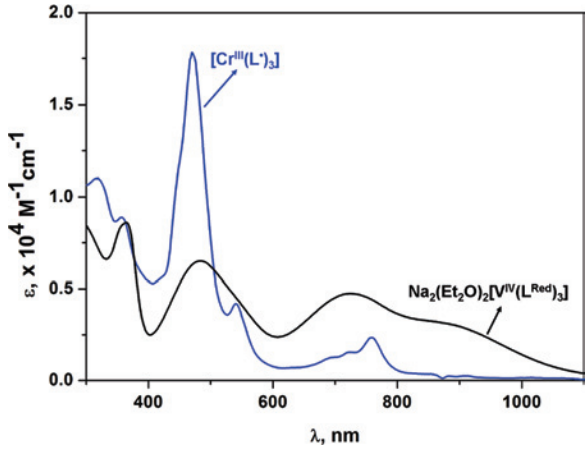

Figure 4. Electronic spectra of **1** in C_6H_6 and **2** in Et_2O.

ground state.[41] The electronic absorption spectrum of **2** in Et_2O (Figure 4) resembles that observed for $[Et_3NH]_2[V^{IV}(cat)_3]$ in MeCN,[9] displaying at least three broad overlapping charge transfer bands in the visible to near IR region (870, 725, and 485 nm). These are ligand-to-metal charge transfer (LMCT) bands, with the two lowest-energy transitions defined as the $a'_2 \rightarrow a'_1$ and $e' \rightarrow a'_1$, respectively (Figure 10).[42,43] The position of these transitions, ~4000 cm^{-1} lower in energy than the corresponding bands in $[V(cat)_3]^{2-}$, underscores the electronic differences between catecholates and aliphatic diketonates.

Temperature-dependent magnetic susceptibility measurements of **2** (Figure 5) display a temperature-independent $\mu_{eff} = 1.72\ \mu_B$ in the range of 4−300 K, which is indicative of the $S = {}^1/_2$ ground state for a V^{IV} d^1 center. The experimental data were corrected for temperature-independent paramagnetism, χ_{TIP}, of -408×10^{-6} cm^3 mol^{-1}. Very weak

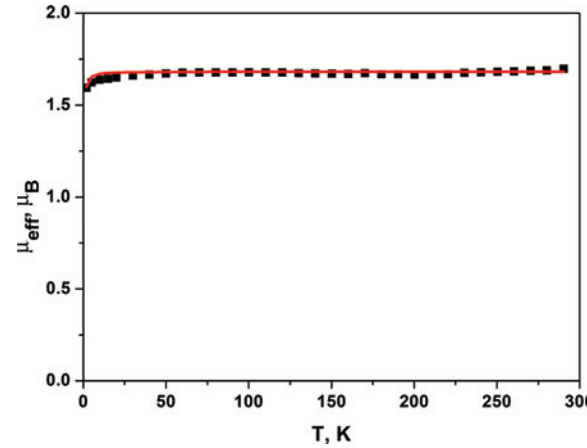

Figure 5. Temperature dependence of the magnetic moment, μ_{eff}, μ_B, of **2**. The solid line represents the best fit to a model described in the text. Black squares are the experimental data.

intermolecular coupling was considered by introducing a Weiss constant, θ, of −0.14 K to account for the low-temperature drop of μ_{eff}. The spectrum was simulated with an isotropic g value of 1.983, identical to the average g value from the X-band EPR spectrum.

Six-coordinate vanadium(IV) complexes are known to fall into two classes. The first class consists of complexes with a $(d_{xy})^1$ configuration, typical of vanadyl $[VO]^{2+}$ moieties. Their EPR spectra display all $g < 2$ and a large ^{51}V (I = 7/2, 100%) hyperfine coupling that generally exceeds 100 $\times 10^{-4}$ cm^{-1}.[44] The second class involves a $(d_{z^2})^1$ ground state corresponding to a trigonal prismatic ligand field with the d_{z^2} essentially nonbonding and independent of the covalent character of the bonding orbitals.[45] The principle spin Hamiltonian parameters display a $g_z \approx 2$, g_x, $g_y < 2$ and $A_{zz} \ll A_{xx}$, A_{yy} pattern with $\langle A \rangle$ considerably less than those of the first class of V^{IV} compounds. The EPR spectrum for **2** (Figure 6) clearly corresponds to this second $(d_{z^2})^1$ ground state configuration with the simulation affording spin Hamiltonian values of $g_z = 2.009$, $g_x = g_y = 1.971$, $A_{zz} = 20 \times 10^{-4}$ cm^{-1}, and $A_{xx} = A_{yy} = 107 \times 10^{-4}$ cm^{-1}. The spectrum of analogous $[Et_3NH]_2[V^{IV}(cat)_3]$ in MeCN shows a similar pattern of principle spin Hamiltonian values, suggesting that both complexes have the same ground-state composition.[9] Formation of $[V^{IV}(cat)_3]^{2-}$ in aqueous solution afforded spectral features similar to those of its powder spectrum, though the latter suffered from significant line broadening inherent to nonmagnetically diluted compounds. It was concluded that irrespective of the solvent and counterions the same EPR spectrum was recorded and that the solid-state geometry was retained in solution.[46] However,

(34) Morosin, B. *Acta Crystallogr., Sect. B* **1965**, *19*, 131.
(35) Pierpont, C. G.; Downs, H. H. *J. Am. Chem. Soc.* **1976**, *98*, 4834.
(36) Buchanan, R. M.; Kessel, S. L.; Downs, H. H.; Pierpont, C. G.; Hendrickson, D. N. *J. Am. Chem. Soc.* **1978**, *100*, 7894.
(37) Sofen, S. R.; Ware, D. C.; Cooper, S. R.; Raymond, K. N. *Inorg. Chem.* **1979**, *18*, 1736.
(38) Downs, H. H.; Buchanan, R. M.; Pierpont, C. G. *Inorg. Chem.* **1979**, *18*, 1736.
(39) Buchanan, R. M.; Clafin, J.; Pierpont, C. G. *Inorg. Chem.* **1983**, *22*, 2552.
(40) Sokolowski, A.; Bothe, E.; Bill, E.; Weyhermüller, T.; Wieghardt, K. *Chem. Commun.* **1996**, 1671.
(41) Benelli, C.; Dei, A.; Gattechi, D.; Güdel, H. U.; Pardi, L. *Inorg. Chem.* **1989**, *28*, 3089.
(42) Karpishin, T. B.; Stack, T. D. P.; Raymond, K. N. *J. Am. Chem. Soc.* **1993**, *115*, 182.
(43) Karpishin, T. B.; Gebhard, M. S.; Solomon, E. I.; Raymond, K. N. *J. Am. Chem. Soc.* **1991**, *113*, 2977.
(44) Mabbs, F. E.; Collison, D. *Electron Paramagnetic Resonance of d Transition Metal Compounds*; Elsevier: Amsterdam, 1992.
(45) (a) Diamantis, A. A.; Raynor, J. B.; Rieger, P. H. *J. Chem. Soc., Dalton Trans.* **1980**, 1731. (b) Chun, H.; Verani, C. N.; Chaudhuri, P.; Bothe, E.; Bill, E.; Weyhermüller, T.; Wieghardt, K. *Inorg. Chem.* **2001**, *40*, 4157.
(46) Branca, B.; Micera, G.; Dessi, A.; Sanna, D.; Raymond, K. N. *Inorg. Chem.* **1990**, *29*, 1586.

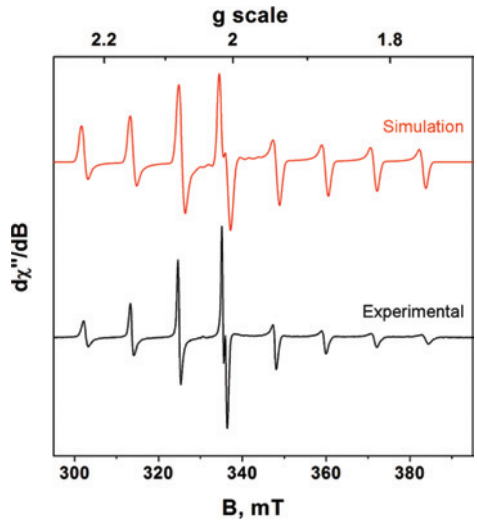

Figure 6. X-band EPR spectrum of **2** in Et_2O at 30 K (frequency = 9.45 GHz, power = 2 μW, modulation amplitude = 5.0 G).

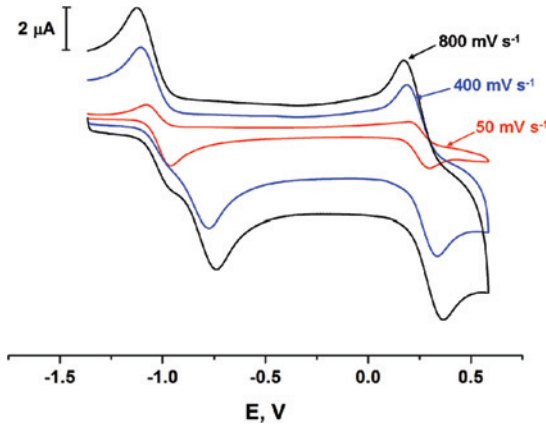

Figure 7. Cyclic voltammogram of **2** in 1:1 Et_2O/CH_2Cl_2 solution (0.10 M $[N(n\text{-}Bu)_4]PF_6$) at 22 °C. Potentials are referenced versus the Fc^+/Fc couple.

as DFT calculations will show, the d_{z^2} ground state persists even for molecules with a large trigonal twist, and as such it is difficult to ascertain solution geometries for these complexes by EPR spectroscopy.

1 proved too unstable to observe any redox processes by cyclic voltammetry, whereas **2** has two quasi-reversible oxidation processes at −1.00 and +0.25 V versus Fc^+/Fc (Figure 7). The first oxidation feature has separated oxidation and reduction waves typical for an EC mechanism. This is ascribed to the loss of a sodium countercation with a possible concomitant geometry change to a more octahedral V^V or V^{IV} species.[10] The UV−vis spectrum of the electrochemically generated monoanion, $[V(L)_3]^{1-}$ (Figure 8), shows three broad, overlapping transitions at 818 nm (ε = 1900 M^{-1} cm^{-1}), 663 nm (ε = 3900 M^{-1} cm^{-1}), and 560 nm (ε = 2000 M^{-1} cm^{-1}). The previously reported catecholate complexes, all assigned as V^V, show similar strong bands in the 600 nm region.[9,47,48] For catechol derivatives, this redox couple can be correlated with the stabilization of higher

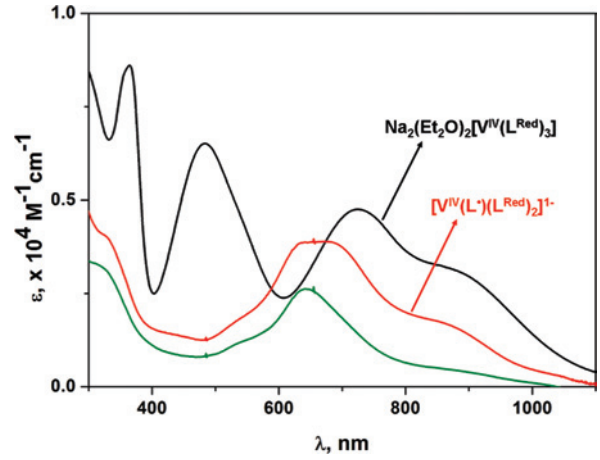

Figure 8. Electronic spectra from the electrochemical oxidation of **2** in 1:1 Et_2O/CH_2Cl_2 solution (0.10 M $[N(n\text{-}Bu)_4]PF_6$) at −20 °C. Oxidation of the monoanionic $[V(L)_3]^{1-}$ species at a potential of +0.4 V produced the green spectrum.

oxidation states by electron-withdrawing substituents.[47] The second oxidation process possibly involves an electronic rearrangement to V^V, V^{IV}, or V^{III} with one, two, or three radical anions, respectively.[9,10] A neutral substituted tris(*o*-semiquinonate) complex $[V^{III}(Cl_4SQ)_3]$ (Cl_4SQ^{1-} = 3,4,5,6-tetrachlorosemiquinonate(1−)) has been proposed to be present in the solid state,[49] although it was thought to undergo an electronic rearrangement to $[V^V(Cl_4SQ)(Cl_4cat)_2]$ (Cl_4cat = 3,4,5,6-tetrachlorocatechol) in solution,[10] with a typical ligand-centered radical g_{iso} of 2.008.[49] Attempts to generate the neutral form of **2** electrochemically were unsuccessful such that further coulometric oxidation of the monoanionic species only depleted it from solution. No new bands were observed in the optical spectrum, suggesting that the second oxidation product is highly unstable and decomposed during the experiment (Figure 8).

Calculations. A depiction of the electronic structures of **1** and **2** was derived from broken symmetry density functional theoretical (BS DFT) calculations using BP86 and B3LYP functionals. Both molecules were truncated with the isopropyl groups replaced by hydrogens to decrease computation time. The geometry of the neutral species in **1** was calculated spin-unrestricted using BS(3,3) with the B3LYP functional. The optimized structure closely resembled the experimental result, with excellent agreement between the experimental and calculated C—O (within ±0.004 Å) and C—C (within ±0.026 Å) bond lengths. There is a slight overestimation of the Cr—O bond lengths (by 0.06 Å), typical for the B3LYP functional, and the experimental twist angle of 40.4° is not quite as accurately reproduced (Θ_{calcd} = 50.0°). Clearly, all three ligands are open-shell, π-radical monoanions as was shown computationally for the analogous $[Fe^{III}(L^{\bullet})_3]$.[18] Three singly occupied orbitals with greater than 90% Cr d-character were identified in the spin-up manifold coupled to three singly occupied ligand orbitals in the spin-down manifold (Supporting Information). These are the defining features of a high spin chromic ion (S_{Cr} = $^3/_2$)

(47) Cass, M. E.; Greene, D. L.; Buchanan, R. M.; Pierpont, C. G. *J. Am. Chem. Soc.* **1983**, *105*, 2680.
(48) Milsmann, C.; Levina, A.; Harris, H. H.; Foran, G. J.; Turner, P.; Lay, P. A. *Inorg. Chem.* **2006**, *45*, 4743.
(49) Buchanan, R. M.; Downs, H. H.; Shorthill, W. B.; Pierpont, C. G.; Kessel, S. L.; Hendrickson, D. N. *J. Am. Chem. Soc.* **1978**, *100*, 4318.

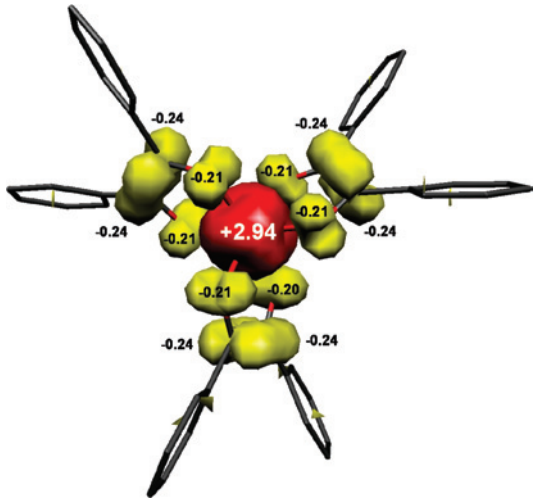

Figure 9. Spin density plot of **1** as derived from BS(3,3) DFT calculations together with the values of the spin density from the Mulliken spin population analysis.

antiferromagnetically coupled to three ligand radical anions to produce a diamagnetic complex ($S = 0$). This notion is further confirmed by the Mulliken spin population analysis (Figure 9)[50] and is very similar to the result calculated for $[Cr^{III}(^{3,6}L^{\bullet}_{sq})_3]$ ($^{3,6}L^{\bullet}_{sq}$ = 3,6-di-*tert*-butylsemiquinonate(1−)).[33]

When the truncated model of **2,** including the two $\{Na(Et_2O)\}^+$ entities, was geometry optimized using a BS(2,1) state and the BP86 functional, an energy minimum was found for an $S = {}^1/_2$ system, although it was not a broken symmetry solution. The agreement between the experimental and calculated V—O bond lengths is again excellent (±0.005 Å). While the intraligand C—O and C—C bond lengths exhibited deviations larger than those observed for **1**, they are clearly indicative of a vanadium(IV) center coordinated by three dianionic ligands $(L^{Red})^{2-}$, yielding a $[V^{IV}(L^{Red})_3]^{2-}$ electronic structure. The trigonal prismatic geometry was not reproduced, with the model twisting a further 26° toward an octahedral geometry ($\Theta_{calcd} = 32.1°$). While the calculated Na···O distances closely match those in the crystal structure (within ±0.03 Å), both the Na···V and Na···OEt_2 distances have shortened by 0.08 Å as a consequence of the trigonal twist. The geometry about each sodium cation changed little after optimization.

The electronic energies and properties of **2** were derived from single-point calculations of the crystallized and optimized geometries using the B3LYP functional. The optimized geometry is significantly more stable than the crystal structure geometry, indicating that the trigonal prismatic geometry results from lattice packing. In fact, removal of the sodium countercations and diethylether solvent molecules only produced a larger twist angle of 41.8°. A very similar twist angle was observed for crystallographically characterized $[Et_3NH]_2[V^{IV}(cat)_3]$.[9,48] A distorted trigonal prismatic geometry ($\Theta = 11.2°$) has been observed for the bicapped complex $[V^{IV}(BCT)]^{2-}$ (BCT = tris(catecholate)ligand bicapped(TRENCAM)).[42] An investigation of a series of complexes with this ligand found that this trigonal prismatic geometry was only observed in complexes with available empty d-orbitals. It was proposed that, combined with an enforced distortion from octahedral geometry due to the catecholate bite angle,[51] π-bonding between the oxygen p_π-orbitals and low-lying d-orbitals (of appropriate symmetry) of the metal was the dominant factor controlling the geometry.

A qualitative molecular orbital (MO) scheme composed of quasi-restricted orbitals of **2** with optimized octahedral geometry is displayed in Figure 10 and clearly shows that the singly occupied molecular orbital (SOMO) is the vanadium d_{z^2} orbital. A Mulliken spin population analysis (Figure 10) identified 1.32 unpaired electrons on the vanadium, which is in agreement with a $(d_{z^2})^1$ ground state but indicative of significant spin polarization that stems from the e' MOs. We will assume **2** is of D_{3h} symmetry; thus, the SOMO transforms as a'_1, while the remaining four d-orbitals comprise the two empty sets of antibonding $(e')^*$ $(d_{x^2-y^2,xy})$ and $(e'')^*$ $(d_{xz,yz})$ MOs. The highest-energy ligand-centered orbital transforms as a'_2, and the bonding equivalents of the LUMO state transform as e'. Transitions from these MOs to the SOMO result in the first two LMCT bands observed in the electronic absorption spectrum. The difference in energy between these orbitals can be indicative of the geometry as twisting stabilizes a'_2 due to a reduction in interligand repulsion, while the e' MOs are destabilized because of reduced metal−ligand π-overlap.[42,43,52,53] The optimized structure and EPR spectrum of **2** are very similar to the crystallographically characterized $(PPh_4)_2[V(mnt)_3]$ (mnt = maleonitriledithiolate; $\Theta = 38°$),[54] which is described as V^{IV} bound by three dianionic dithiolene ligands. It appears that even large deviations from trigonal prismatic geometry have little impact on the electronic structure of the complex, and thus the vanadium d_z^2 orbital is the SOMO for both $[Et_3NH]_2[V^{IV}(cat)_3]$ and **2**, despite the former being more octahedral in the solid state.[46]

Geometry optimizations were also carried out on the one- and two-electron oxidized forms of **2**. In both cases, optimization started from the truncated **2** with the sodium atoms and diethylether molecules removed. For the singly oxidized monoanionic product, the lowest-energy solution was found using a BS(1,1) state with the B3LYP functional. Only one ligand is an open-shell π-radical monoanion coupled to one singly occupied metal d-orbital. This solution is 9.2 kcal mol^{-1} more favorable than the closed-shell singlet solution and describes a $[V^{IV}(L^{\bullet})(L^{Red})_2]^{1-}$, containing a V^{IV} ($S_V = {}^1/_2$) center rather than V^V ($S_V = 0$), which has been reported for catechol systems.[9,10,48] The molecule is clearly octahedral with a calculated twist angle of 37°. The crystal structure of $Na[V(cat\text{-}3,5\text{-}^tBu_2)_3]\cdot 4CH_3OH$ is the only structurally characterized monoanionic vanadium tris(catecholate)

(50) Herebian, D.; Wieghardt, K.; Neese, F. *J. Am. Chem. Soc.* **2003**, *125*, 10997.
(51) Raymond, K. N.; Isied, S. S.; Brown, L. D.; Fronczek, F. R.; Nibert, J. H. *J. Am. Chem. Soc.* **1976**, *98*, 1767.
(52) Hoffmann, R.; Howell, J. M.; Rossi, A. R. *J. Am. Chem. Soc.* **1976**, *98*, 2484.
(53) Tenderholt, A. L.; Szilagyi, R. K.; Holm, R. H.; Hodgson, K. O.; Hedman, B.; Solomon, E. I. *Inorg. Chem.* **2008**, *47*, 6382.
(54) Kwik, W.-L.; Stiefel, E. I. *Inorg. Chem.* **1973**, *12*, 2337.

species.[10,55] The complex crystallizes as a dimer, bridged by Na countercations and solvent molecules. Geometry optimization of $[V(cat)_3]^{1-}$ was carried out using a singlet ($M_S = 1$), triplet ($M_S = 3$), and BS(1,1) states. All optimizations produced near identical geometries and very similar total energies. The lowest-energy solution was BS(1,1), although it was only 2 kcal mol^{-1} lower than the singlet state and 2.4 kcal mol^{-1} lower than the triplet state. These values are within the error limits for DFT and make a definitive assignment ambiguous. However, vanadium K-edge X-ray absorption spectroscopy (XAS) studies explicitly show a V^V center, and therefore, we define this molecule as $[V^V(cat)_3]^{1-}$.[48]

A qualitative MO scheme of $[V^{IV}(L^{\bullet})(L^{Red})_2]^{1-}$ is presented in Figure 11 and shows weak antiferromagnetic coupling between the a'_1 (d_{z^2}) and ligand-centered a'_2 MOs. These orbitals are near orthogonal and have a very low orbital overlap integral (S = 0.0002), suggesting they are uncoupled. The triplet state ($S = 1$) is only 4.1 kcal mol^{-1} higher in energy than that of the BS solution. This difference in electronic structure between our monoanion and its catechol equivalent can be ascribed to a difference in the reduction potential of the bound π-radical monoanion for aromatic and aliphatic 1,2-diketones; the $[V(cat)_3]^{1-}/[V(cat)_3]^{2-}$ redox potential is ~500 mV more positive than for **2**.[9,48] A Mulliken spin population analysis identified +1.81 unpaired electrons at vanadium with a similar amount of negative electron spin density distributed on the three ligands (Figure 11), which is the result of significant spin-polarized covalent bonding. The Löwdin spin population of the vanadium $d_{x^2-y^2,xy}$ orbitals has increased 3-fold compared to that of **2** because of significantly increased metal−ligand overlap in the e' MOs.

The geometry-optimized, doubly oxidized neutral complex from **2** afforded a broken symmetry BS(3,2) solution using the B3LYP functional. The resultant structure is clearly octahedral ($\Theta = 35.7°$) with considerably longer V−O bond distances (av 2.004 Å) compared to those of **2** and the optimized monoanion. The qualitative MO scheme (Figure 12) shows three ligand-centered SOMOs in the spin up manifold and two vanadium SOMOs in the spin down manifold ($S_V = 1$). The two vanadium SOMOs are antiferromagnetically coupled with two ligand orbitals with an orbital overlap integral of S = 0.55. Thus, the neutral species is defined as $[V^{III}(L^{\bullet})_3]$ with a ligand-centered doublet ($S = {}^1/_2$) ground state. This calculated result is directly analogous to the electronic structure for **1**. This notion is further confirmed by the Mulliken spin population analysis (Figure 12) that shows two electrons on vanadium and three electrons distributed over the ligands. Violet crystals of $V(catCl_4)_3$ exhibited unit cell parameters very similar to those of the structurally characterized $Cr(Cl_4SQ)_3$ and $Fe(Cl_4SQ)_3$.[10] However, a false inversion symmetry at the origin precluded a successful refinement of the structure. Regardless, it is defined as $[V^{III}(Cl_4SQ)_3]$ based on IR and EPR results,[10] and

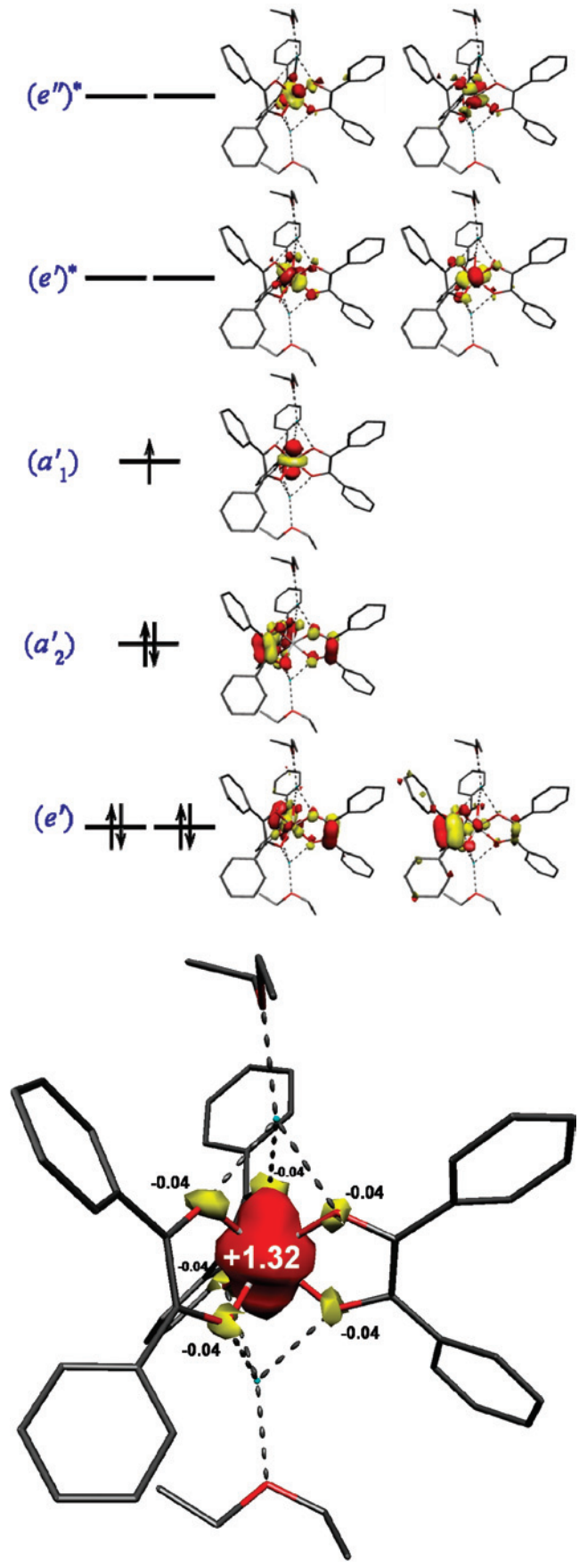

Figure 10. Qualitative MO scheme (top) and spin density plot (bottom) of **2** together with values of the spin density of the Mulliken spin population analysis.

(55) Yin, C.-X.; Finke, R. G. *J. Am. Chem. Soc.* **2005**, *127*, 9003.

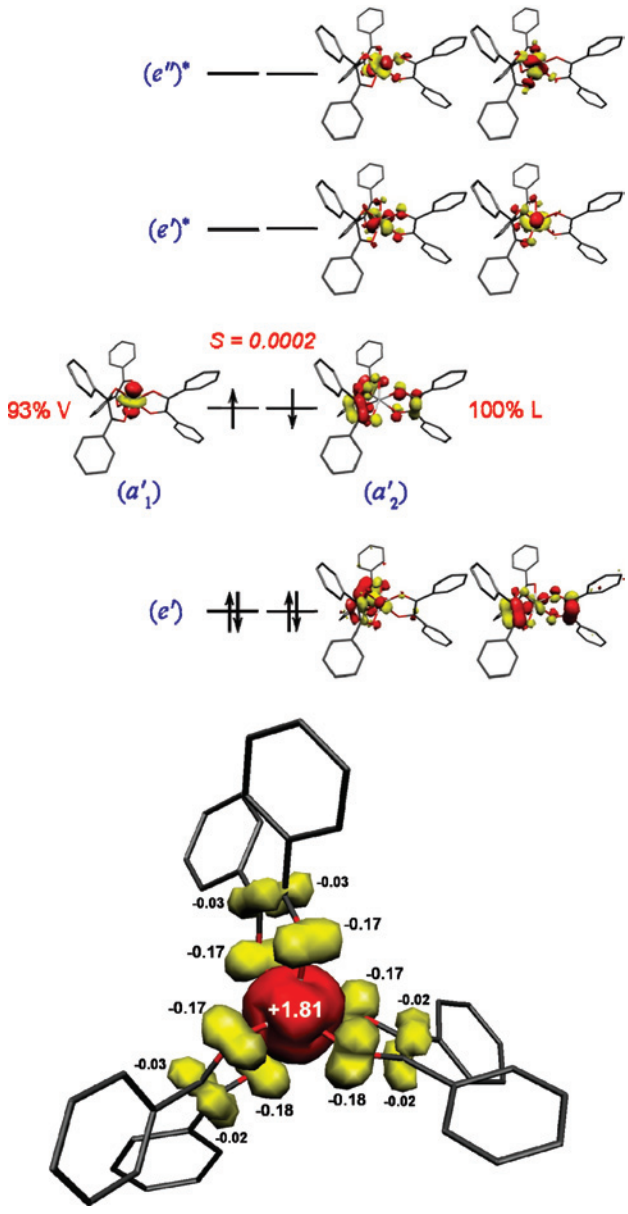

Figure 11. Qualitative MO scheme (top) and spin density plot (bottom) of $[V^{IV}(L^{\bullet})(L^{Red})_2]^{1-}$ together with values of the spin density of the Mulliken spin population analysis.

it is rewarding to see the same electronic structure has been found in our calculations for $[V^{III}(L^{\bullet})_3]$.

Conclusions

The bulky diaryl 1,2-diketone bis(2,6-diisopropylphenyl)glyoxal $(L^{Ox})^0$ is a redox active ligand that can also form complexes in its doubly reduced closed-shell $(L^{Red})^{2-}$ state or as a singly reduced π-radical anion $(L^{\bullet})^{1-}$. From a combination of structural and spectroscopic investigations in conjunction with broken symmetry DFT calculations, it has been possible to unequivocally establish the electronic structures for two early transition metal complexes, namely, octahedral $[Cr^{III}(L^{\bullet})_3]^0$ (**1**) and trigonal prismatic $Na_2(Et_2O)_2$-$[V^{IV}(L^{Red})_3]$ (**2**). Neutral **1** contains a high spin chromic ion ($S_{Cr} = {}^3/_2$) coupled to three ligand radical anions leading to an $S = 0$ ground state and is essentially identical to the well-characterized neutral Cr complexes with catecholate ligands.

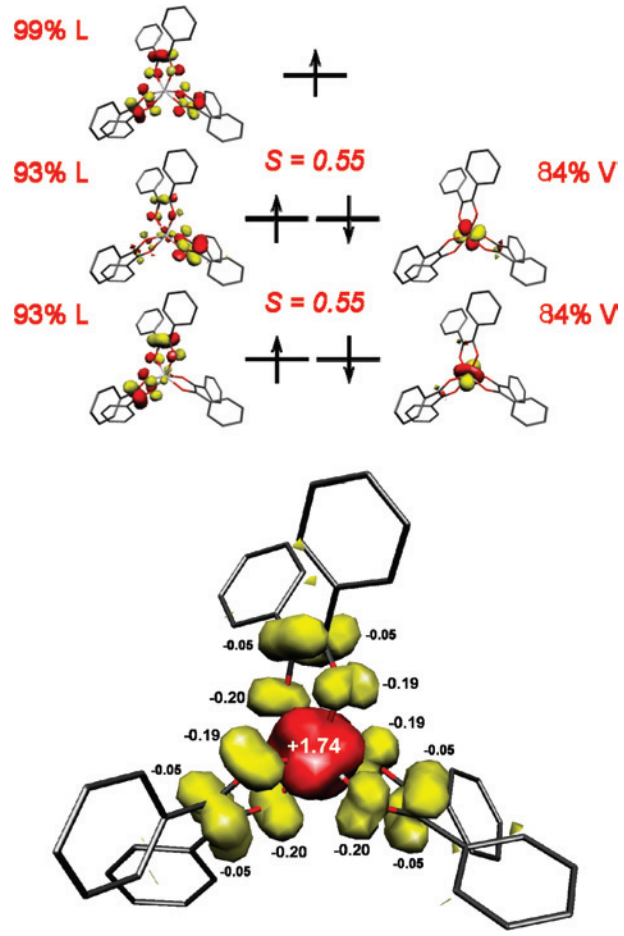

Figure 12. Qualitative MO scheme (top) and spin density plot (bottom) of $[V^{III}(L^{\bullet})_3]^0$ together with values of the spin density of the Mulliken spin population analysis.

Pierpont et al. have described the seven-membered electron transfer series $[Cr(cat)_3]^z$ ($z = 3+, 2+, 1+, 0, 1-, 2-, 3-$) as entirely ligand-based redox processes with the central ion remaining in the +III oxidation state.[38] This conclusion was supported by Fenske−Hall molecular orbital calculations[56] and demonstrates that the $(t_{2g})^3$ electron configuration is highly favored by chromium. In contrast, the dianion in **2**, $[V^{IV}(L^{Red})_3]^{2-}$, contains a d^1 V^{IV} ion with three closed-shell ligands, $(L^{Red})^{2-}$ ($S = {}^1/_2$). The VO_6 trigonal prism is capped at either end by a Na countercation and crystallizes with a twist angle of 6.1°, although DFT calculations infer that this is the result of lattice packing. The one-electron oxidation of **2** is proposed to be ligand-centered with the concomitant loss of Na countercation interactions and a twist to more octahedral geometry. This species is formulated as $[V^{IV}(L^{\bullet})(L^{Red})_2]^{1-}$, containing a V^{IV} ($S_V = {}^1/_2$) center, antiferromagnetically coupled to one singly reduced radical anion rather than V^V ($S_V = 0$) as in the case of the catechol analogue. This difference in electronic structure can be ascribed to a difference in the reduction potential of the bound π-radical monoanion for aromatic and aliphatic 1,2-diketones. DFT calculations suggest a two-electron oxidation

(56) Gordon, D. J.; Fenske, R. F. *Inorg. Chem.* **1982**, *21*, 2907.

of **2** produces a V^{III} center ($S_V = 1$) coupled to three ligand radical anions $[V^{III}(L^{\bullet})_3]^0$. This species has a ligand-based SOMO and is isostructural with **1**.

The first molecular complexes with trigonal prismatic geometry were those with analogous dithiolene ligands, specifically, $Re(S_2C_2Ph_2)_3$,[57] $Mo(edt)_3$ (edt = ethene-1,2-dithiolate),[58] and $V(S_2C_2Ph_2)_3$.[59] Trigonal prismatic geometry is most prevalent for tris(dithiolene) complexes of the early transition metals V, Mo, W, and Re,[60] although there are several examples with oxygen-donor,[61] nitrogen-donor,[62] and organometallic ligands.[63] Various factors, including metal oxidation state, interligand bonding, metal and ligand orbital energies, lattice packing, and overall complex charge, have been suggested to stabilize trigonal prismatic geometry in preference to octahedral geometry.[52,60−62,64−66] Interestingly, neutral $V(S_2C_2Ph_2)_3$ is trigonal prismatic, while its diketonate counterpart is calculated as octahedral. The former has an EPR spectrum indicative of a $(d_{z^2})^1$ ground state with the ^{51}V hyperfine similar to $[V(mnt)_3]^{2-}$ and **2**.[54] The lack of trigonal prismatic geometry in V(diketonate)$_3$ can be ascribed to a difference in energy of oxygen 2p orbitals compared to sulfur 3p orbitals relative to the vanadium 3d orbitals. Out-of-plane sulfur 3p orbitals have greater overlap with the $d_{x^2-y^2}$ and d_{xy} orbitals (e') (Figure 10) stabilizing a trigonal prism that can be further supported by interligand S−S bonds.[64,67] By definition, $V(S_2C_2Ph_2)_3$ must contain oxidized ligands for charge balance. This manifests as an empty a'_2 orbital that favors interligand bonding through the lowering of ligand−ligand repulsion. In contrast, V(diketonate)$_3$ has the energetically favored $(t_{2g})^3$ configuration and weaker 2p−3d π-overlap, which results in an octahedral coordination sphere with three ligand radicals. Based on similar X-ray powder diffraction patterns and electronic absorption spectra to $V(S_2C_2Ph_2)_3$ and $Mo(S_2C_2Ph_2)_3$, $Cr(S_2C_2Ph_2)_3$ is purported to also possess trigonal prismatic geometry.[57,59,68] However, in a D_{3h} ligand field there would be one electron in the metal-centered $(e')^*$ MO, for a Cr^{III} d^3 ion, that is antibonding with respect to a trigonal prism and forces the geometry octahedral. Therefore, a higher oxidation state for chromium (IV−VI) is needed to maintain a trigonal prismatic structure. While **1** clearly contains a Cr(III) central ion with the favorable $(t_{2g})^3$ configuration, it remains to be seen whether dithiolene ligands can stabilize the high Cr oxidation state necessary to produce a neutral trigonal prismatic complex.

Acknowledgment. G.H.S. thanks the Alexander von Humboldt Foundation for a fellowship, and S.S. is grateful to the Max-Planck Society for a stipend. We are grateful for financial support from the Fonds der Chemischen Industrie.

Supporting Information Available: X-ray crystallographic information for the two compounds in Table 1, NMR spectra for **1**, cyclic voltammetry for **1**, and the free ligand $(L^{Ox})^0$. Also, further details of DFT calculations with a MO scheme for **1**. This material is available free of charge via the Internet at http://pubs.acs.org.

IC801122M

(57) Eisenberg, R.; Ibers, J. A. *J. Am. Chem. Soc.* **1965**, *87*, 3776.
(58) Smith, A. E.; Schrauzer, G. N.; Mayweg, V. P.; Heinrich, W. *J. Am. Chem. Soc.* **1965**, *87*, 5798.
(59) Eisenberg, R.; Gray, H. B. *Inorg. Chem.* **1967**, *6*, 1844.
(60) Beswick, C. L.; Schulman, J. M.; Stiefel, E. I. *Prog. Inorg. Chem.* **2004**, *52*, 55.
(61) (a) Kepert, D. L. *Prog. Inorg. Chem.* **1977**, *23*, 1. (b) Pierpont, C. G.; Buchanan, R. M. *J. Am. Chem. Soc.* **1975**, *97*, 4912. (c) McMurry, T. J.; Hosseini, M. W.; Garrett, T. M.; Hahn, F. E.; Reyes, Z. E.; Raymond, K. N. *J. Am. Chem. Soc.* **1987**, *109*, 7196.
(62) (a) Wentworth, R. A. D. *Coord. Chem. Rev.* **1972**, *9*, 171. (b) Fleischer, E. B.; Gebala, A. E.; Swift, D. R.; Tasker, P. A. *Inorg. Chem.* **1972**, *11*, 2775. (c) Comba, P.; Sargeson, A. M.; Engelhardt, L. M.; Harrowfield, J. M.; White, A. H.; Horn, E.; Snow, M. R. *Inorg. Chem.* **1985**, *24*, 2325.
(63) (a) Kaupp, M. *J. Am. Chem. Soc.* **1996**, *118*, 3018. (b) Morse, P. M.; Girolami, G. S. *J. Am. Chem. Soc.* **1989**, *111*, 4114. (c) Kaupp, M.; Kopf, T.; Murso, A.; Stalke, D.; Strohmann, C.; Hanks, J. R.; Cloke, F. G. N.; Hitchcock, P. B. *Organometallics* **2002**, *21*, 5021. (d) Vaid, T. P.; Veige, A. S.; Lobkovsky, E. B.; Glassey, W. V.; Wolczanski, P. T.; Liable-Sands, L. M.; Rheingold, A. L.; Cundari, T. R. *J. Am. Chem. Soc.* **1998**, *120*, 10067.
(64) Stiefel, E. I.; Eisenberg, R.; Rosenberg, R. C.; Gray, H. B. *J. Am. Chem. Soc.* **1966**, *88*, 2956.
(65) Kang, S. K.; Tang, H.; Albright, T. A. *J. Am. Chem. Soc.* **1993**, *115*, 1971.
(66) Chisholm, M. H.; Parkin, I. P.; Streib, W. E.; Eisenstein, O. *Inorg. Chem.* **1994**, *33*, 812.
(67) Pierpont, C. G.; Eisenberg, R. *J. Chem. Soc. A* **1971**, 2285.
(68) Eisenberg, R.; Stiefel, E. I.; Rosenberg, R. C.; Gray, H. B. *J. Am. Chem. Soc.* **1966**, *88*, 2874.